ANALYSIS OF THIN-WALLED GIRDERS SUBJECTED TO A PULSE TORSIONAL TORQUE

Leszek Czechowski, Tomasz Kubiak

Lodz University of Technology
Department of Strength of Materials and Structures
Stefanowskiego Street 1/15, 90-924 Lodz, Poland
tel.: +48 42 6312214, fax: +48 42 6364985
e-mail: leszek.czechowski@p.lodz.pl, tomasz.kubiak@p.lodz.pl

Abstract

Thin-walled structures, which are primarily meant for static load service conditions may be subjected to transient dynamic loads, which may in turn lead to a more dangerous state of stress in the structure. These transient overloads as compared to steady state (static) loads may deteriorate the mechanical properties of the structural member or lead to its failure.

Therefore, analysis of dynamically loaded structures, or the answer to the question at what dynamic loading relative to static loading the structures may be serviceable, is a valid and pertinent issue. This paper deals with thin-walled iso- and/or orthotropic box girders subjected to a pulsed torsional moment causing restrained torsion. Numerical calculations were conducted by means of the ANSYS® software, a computer suite applying the finite element method [12].

The results were presented in the form of displacement maps and diagrams determining the maximum angle of rotation or deflection of the girder wall as a function of the dynamic load factor, DLF (the ratio of pulse loading amplitude to static critical load).

Keywords: thin-walled structures, dynamic buckling, finite element modelling

1. Introduction

The literature on structural stability problems has been developed for over a century and is now very extensive. On the other hand, dynamic (pulse) loading of thin-walled members with flat walls has been discussed only recently – mainly in the context of dynamic buckling of thin-walled members subjected to compressive pulse loads or a bending moment [1, 6, 8]. These papers described the phenomenon of dynamic buckling and presented some criteria for the assessment of the dynamic stability of structural members. In the case of torsional loading, no known publications deal with dynamic loads, even though some papers discuss static loads and analysis of girders throughout their entire working range [2, 4].

For many years now, the stability of thin-walled structural members subjected to static torsion has been studied both theoretically and empirically, which has resulted in a substantial body of literature on the subject. Some papers exploring dynamic stability under the influence of a torsional moment are devoted to thin-walled cylindrical shells (e.g. in [7, 9-11]), but there are no works dealing with thin-walled girders. The still insufficient knowledge regarding this area was the motivation for assessing the behaviour of thin-walled structural members of various types (mostly plate structures) under the influence of pulse torsional loads.

In the present paper, the authors analyze dynamic buckling, that is, the behaviour of a structure under pulse loading whose duration equals (or approximates) the fundamental natural vibration period of the structure in question. Numerical calculations were conducted to determine the dynamic response of such structures to rectangular pulse loading. The considered thin-walled girder cross-sections included regular 4-, 6-, 12-, and 20-sided polygons inscribed in a circle of the same diameter and an isosceles trapezoidal cross-section. For the studied structures, an isotropic or

orthotropic linear-elastic model of material was adopted with the assumption that in orthotropic material the main directions of moduli coincided with the edges of the girder walls.

2. Girder shape and material

The study focuses on girders composed of plates with an even number of sides (4, 6, 12, 20) whose polygons are inscribed in a circle (Fig. 1) of the same diameter *2R*. Also a girder with an isosceles trapezoidal cross-section is studied, with the dimensions presented in Fig. 2. The material properties used in the calculations are shown in Tab. 1. For regular polyhedrons, the adopted material properties were marked as steel/mat_1 and all mat_2, while for trapezoid girders – steel/mat_1 and orthotropic material properties marked as mat_3.
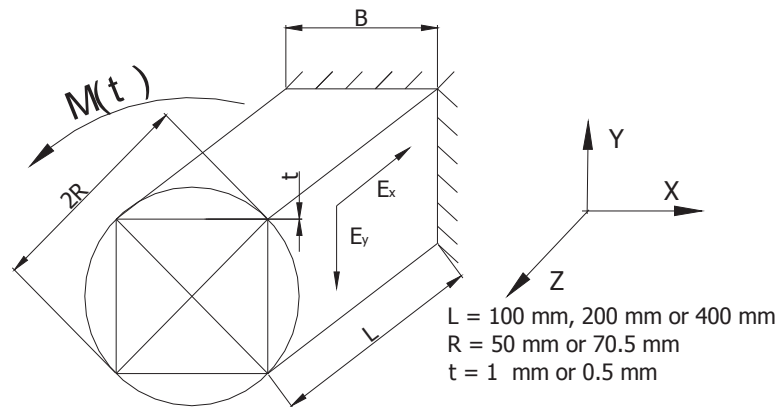

L = 100 mm, 200 mm or 400 mm
R = 50 mm or 70.5 mm
t = 1 mm or 0.5 mm

Fig. 1. Drawing of the one of four considered columns with dimensions and directions of elastic module

Tab. 1. Material constants

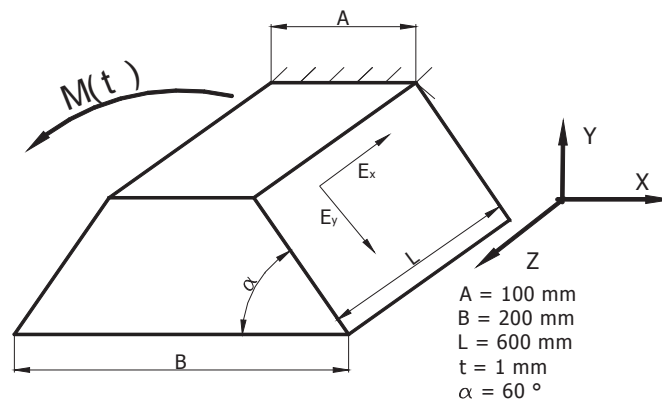| Material	E_x [GPa]	E_y [GPa]	v_{yx} [−]	G [GPa]	ρ[kg/m^3]
steel/mat_1	200	200	0.3	80	7800
mat_2_1	29.523	97.423	0.3	11.818	2000
mat_2_2	97.423	29.523	0.09	11.818	2000
mat_3_1	30	15	0.15	10	7800
mat_3_2	30	60	0.3	10	7800
mat_3_3	30	30	0.3	10	7800

A = 100 mm
B = 200 mm
L = 600 mm
t = 1 mm
α = 60 °

Fig. 2. Dimensions of column with trapezium cross-section

3. Numerical simulation

3.1. Structures subjected to restrained torsion

In numerical simulations, an eight-node shell element with six degrees of freedom at each node (Fig. 3).
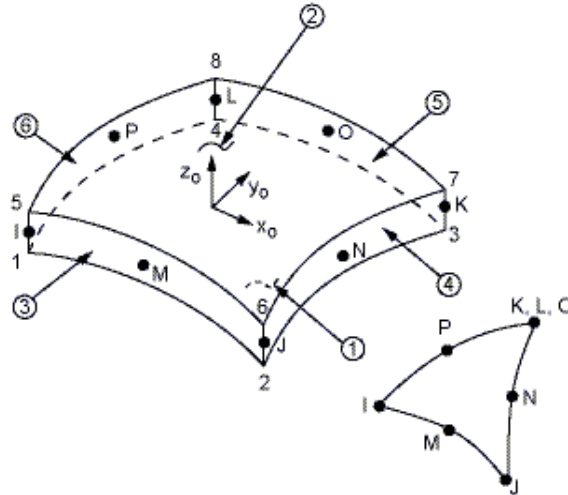

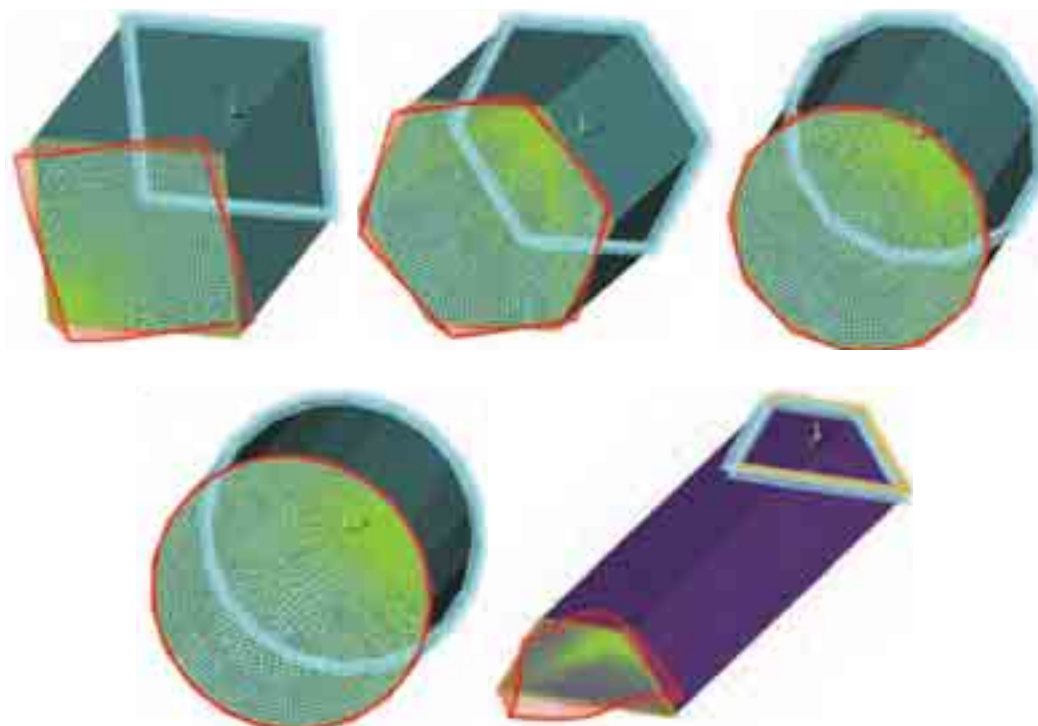*Fig. 3. Element type shell281 used in analysis [12]*

Fig. 4. Discrete models of girders subjected to torsion

Discrete models of the considered girders are presented in Fig. 4, which show not only the element mesh, but also boundary conditions and loads. Along the edges of one end of the girder, zero values of displacement along all directions were adopted (restraint), while at nodes situated at the opposite end of the girder, a load corresponding to the torsional moment was applied, which was implemented by uniform distribution of the forces applied at the nodes along the free edges within a cylindrical system of coordinates adopted for these nodes. To ensure that the edges of the girder are straight, a transverse plate was introduced to the model in the plane in which the load

was applied, which was several times thicker than the other girder walls. The pulse loading was of rectangular nature, with its duration equal to the fundamental natural vibration period of the considered structure.

3.2. Determination of the maximum angle of rotation and deflection

For a girder of square cross-section, analysis was conducted by two methods: the maximum angle of rotation of the free end or deflection in the middle of the plates was determined throughout the entire range of the pulse action. For the other cross-sections, only the maximum angle of rotation as a function of dynamic loading was found.
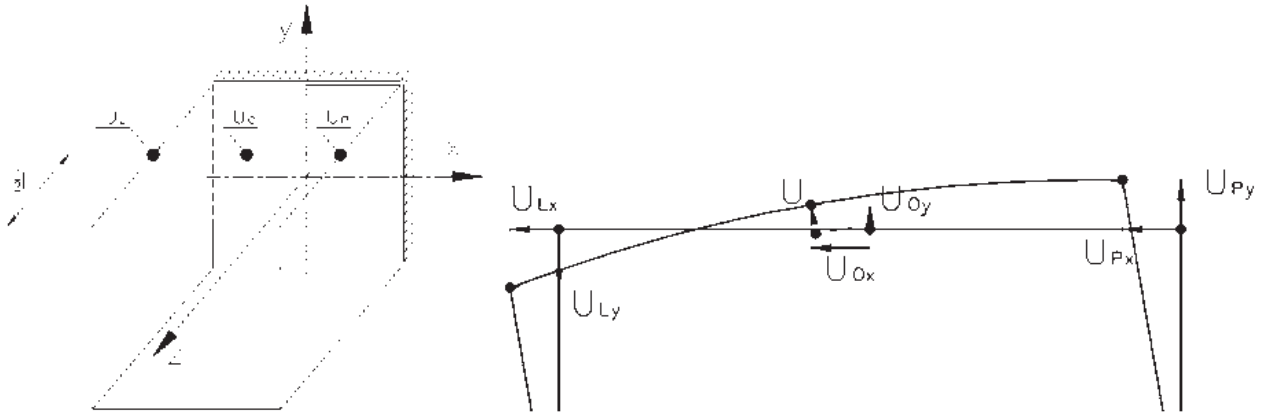

Fig. 5. The way of measurment of wall deflection (buckling)

Deformation analysis of the walls of the girder subjected to torsion is non-trivial, because the displacement of a given node in the discrete model involves the displacement related to the rotation of the cross-section and the displacements (girder wall deformation) related to loss of stability (wall deflection). The displacement of any given point on the cross-section may be determined from the following equation:

$$u_{abs} = \sqrt{u_{Ox}^2 + u_{Oy}^2} \ , \tag{1}$$

assuming that the considered point on the cross-section lies in the plane of the cross-section after deformation. It should be remembered that the displacement determined in this way contains the displacement related to the rotation of the structure and the deflection of the wall. In order to separate the above-mentioned displacements, it was assumed that the displacement of any point on the cross-section along the normal direction of that cross-section may be neglected, and, in the case where stability is not lost, the cross section remains a polygon before and after the rotation (its edges remain straight after the rotation – Fig. 5). The assumption that the edges of the cross-section remain straight makes it possible to determine the vertical u_{av_y} and horizontal u_{av_x} displacements for a point located on a given cross-section halfway between two corners, using the following equations:

$$u_{av\_x} = \tfrac{1}{2}\left(u_{Lx} + u_{Px}\right), \ u_{av\_y} = \tfrac{1}{2}\left(u_{Ly} + u_{Py}\right), \tag{2}$$

where:
u_{Lx} - is the horizontal (x) displacement from the left corner (point L in Fig. 5),
u_{Ly} - is the vertical (y) displacement from the left corner (point L in Fig. 5),
u_{Px} - is the horizontal (x) displacement from the left corner (point P in Fig. 5),
u_{Py} - is the vertical (y) displacement from the right corner (point P in Fig. 5).

Displacement related to the deformation of the wall U without taking into consideration the displacement related to the rotation of the cross-section may be found by deducting from the overall displacements u_{Ox} and u_{Oy} those related to rotation u_{av_y} and horizontal displacement u_{av_x} of the point and add geometrically to obtain:

$$U = \sqrt{\left(u_{Ox} - u_{av\_x}\right)^2 + \left(u_{Oy} - u_{av\_y}\right)^2}.$$

(3)

4. Calculation results

4.1. Assessment of stability through measurement of the angle of rotation

Most of the diagrams shown in this section of the paper present the relationship between the maximum angle of rotation of the free end obtained throughout the entire range of the loading as a function of the torsional moment amplitude (Fig. 7-12).
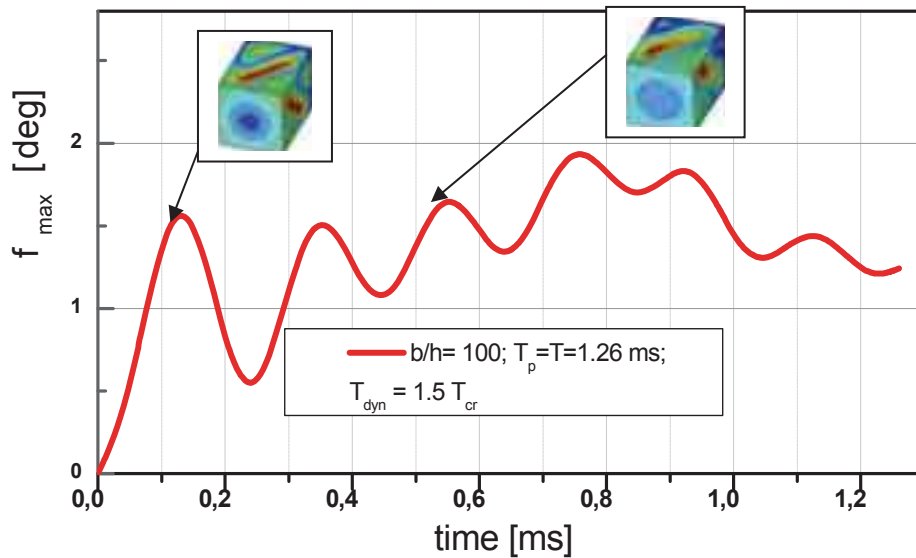

Fig. 6. Course of torsion angle dependent upon the duration of the dynamic torque equals 1.5 T_{cr}

Figure 6 presents a sample course of the angle of rotation of a girder as a function of time of action of the torsional moment for the square cross-section at an overload of 1.5 T_{cr}. The course of the angle changes depending on the dynamic loading, and for low moments (below 1 T_{cr}) the highest angle appeared at 0.2-0.3 T_p of the time of application, while after increasing the amplitude the maximum value was observed at 0.6-0.8 T_p.

For the rectangular cross-section (Fig. 7), it was observed that the thinner the structure was the greater the dynamic torsional moment overload could be (even over twofold for the thickness $t = 0.5$ mm). For moduli along the x axis that were higher than those along the transverse direction, the structure may carry greater dynamic loads (a sharp increase in the angle of rotation appears at 1.7 T_{cr}). Comparing the isotropic material with the composite in which the modulus E_x is smaller than the modulus E_y, it was observed that the boundary dynamic moments remain at the same level, even though in the latter case the angle of rotation is twice as high for the same overload.

The subsequent diagram shows the same relationship (Fig. 8), but for a girder with regular hexagonal cross-section. Calculations were made only for isotropic material, comparing them with the solution for static loading. As can be seen from the figure, the curves obtained for pulse loads are shifted to the left (irrespective of the plate thickness, transient angles of rotation under dynamic

loading are greater than under static loading). In Fig. 9, which presents a diagram for *n* = 12 (the number of girder walls), the course of the curves is similar to Fig. 7 (for E_x/E_y lower than 1, girders can carry lower dynamic loads than in the opposite case). Fig. 10 shows curves for a beam with regular icosagonal cross-section.
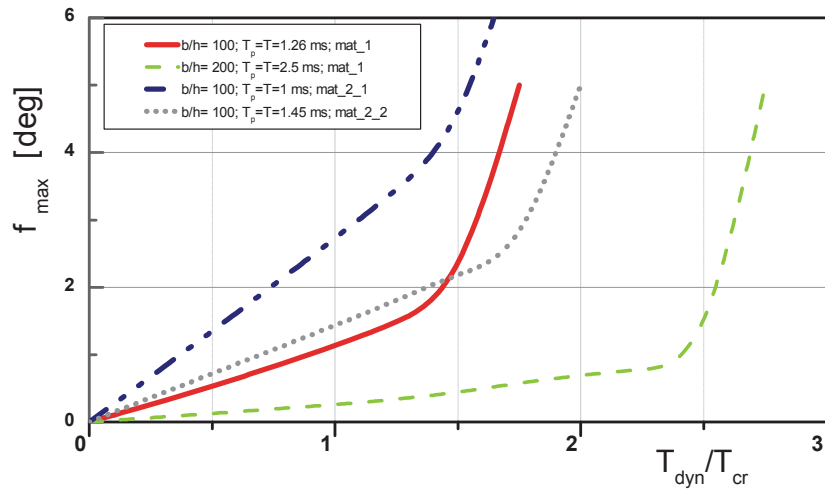

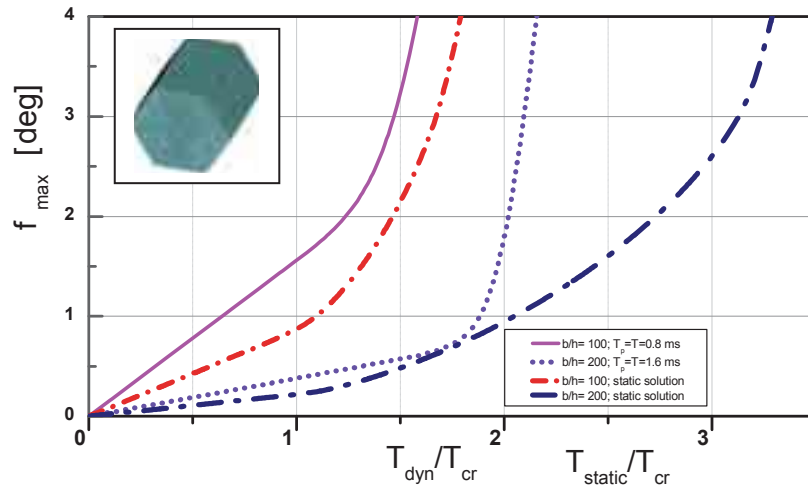*Fig. 7. Maximal angle dependent upon the dynamic torque and the static torque for the number of walls n=4*

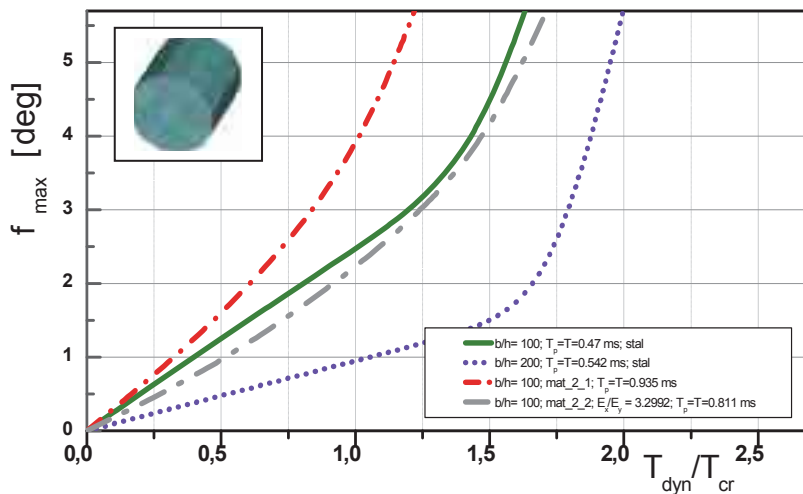*Fig. 8. Maximal angle dependent upon the dynamic torque and the static torque for the number of walls n=6*

Fig. 9. Maximal angle dependent upon the dynamic torque and the static torque for the number of walls n=12

Analyzing the obtained results, it is worth noting that in the case of dynamic loading, a sharp increase in the angle of rotation occurs at a torsional moment that is about half of that for static loadings.
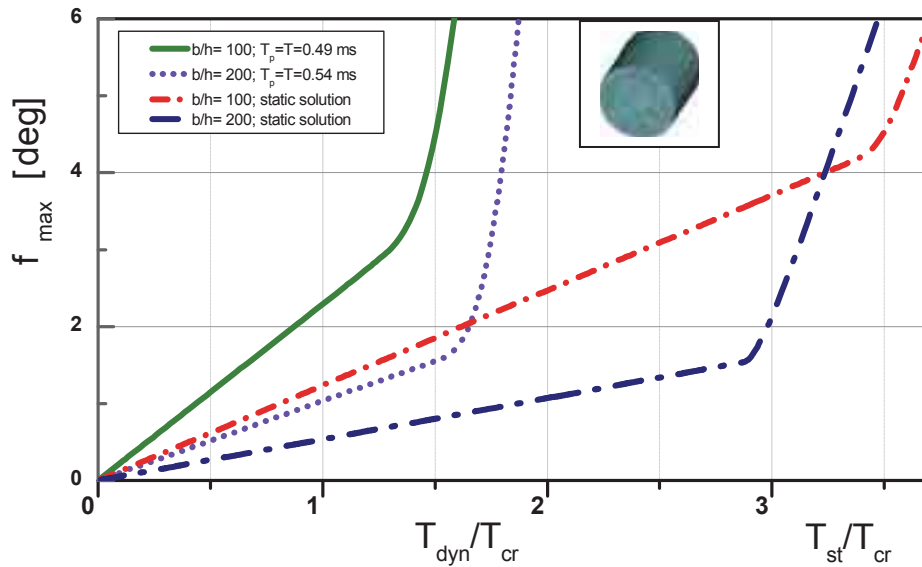

Fig. 10. Maximal angle dependent upon the dynamic torque and the static torque for the number of walls n=20

Figure 11 presents all steel girders with a wall thickness of 1 mm. Differences are not large, although in the case of the hexagonal beam, an abrupt increase in the angle of rotation occurs already at 1.25 T_{cr}, as compared to slightly above 1.35 T_{cr} for the other girders.
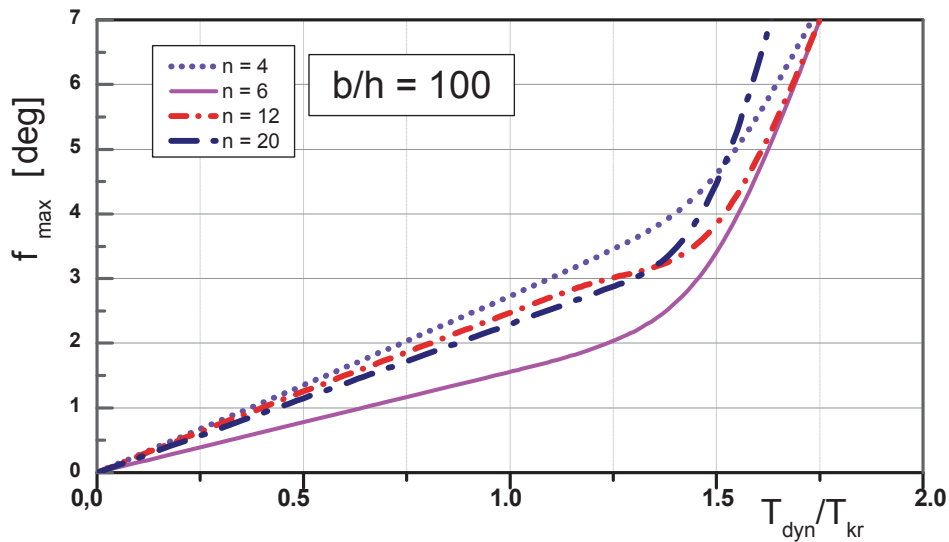

Fig. 11. Maximal angle dependent upon the dynamic torque for different number of walls

Considering the results obtained for girders of trapezoidal cross-section (Fig. 12), it can be seen that all the curves are significantly shifted to the right; in contrast to the results described previously (the studied girders were six times shorter).

Still, the general character of the curves was preserved, as in the case of orthotropic materials (Fig. 7 and 9) in which Young's modulus along the girder axis has a positive influence on the value of the dynamic moment carried. Comparing mat_1 and mat_3_3 (properties of isotropic materials), it seems that they are similar.
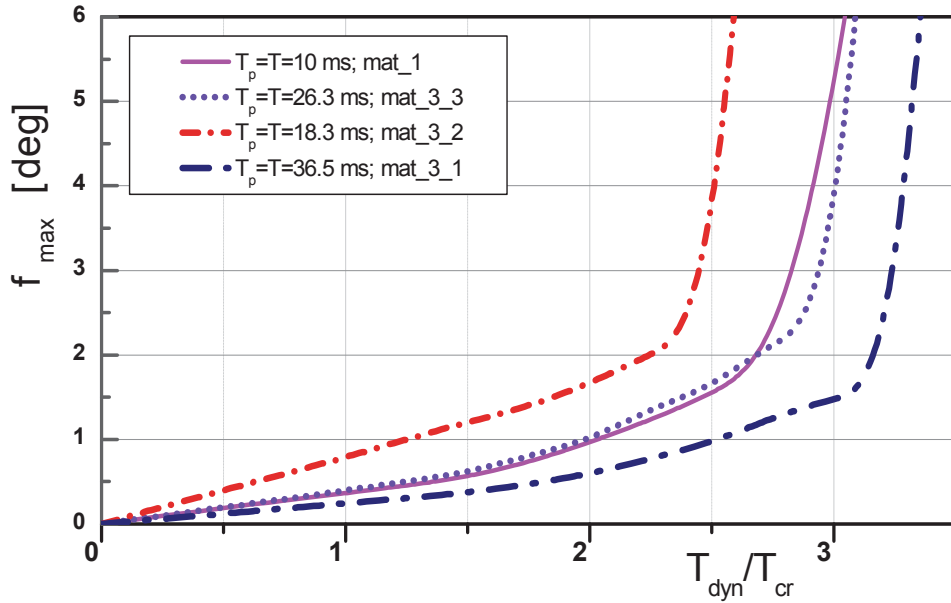
Fig. 12. Maximal angle dependent upon the dynamic torque for columns with trapezium cross-section

4.2. Assessment of dynamic stability through measurement of deflection

This section presents the results of analysis of square cross-section girders with the length l = 100, 200, and 400 mm. Dynamic stability was assessed using adequate criteria [5] and was based on analysis the deflection of the girder wall as a function of the dynamic load factor (DLF) defined as the ratio of pulse loading amplitude to static critical load. Fig. 13 shows dimensionless deflection as a function of DLF for a girder with the length l = 200 mm subjected to a pulse torsional moment. Displacements were measured halfway through the length and width of the upper wall of the girder. Fig. 13 presents four different curves: the first one, marked with the letter U is the curve showing the maximum deflection of the middle of the upper wall of the girder recorded during time t within the range $0 < t < 1.5\ T_p$ (the entire time of analysis of girder deformation) and determined by means of equation (3) as a function of DLF. The second curve, marked U_{imp}, is the maximum deflection of a given point on the girder determined by means of equation (3) based on the deflections recorded throughout the duration of the impulse ($0 < t < T_p$). The other two curves, marked U_0 and U_{0imp}, represent the overall maximum dislocation of the middle of the upper wall of the girder as a function of DLF, and the deflections were determined throughout the duration of the analysis ($0 < t < 1.5\ T_p$) – curve U_0, or throughout the duration of the pulse ($0 < t < T_p$) – curve U_{0imp}.
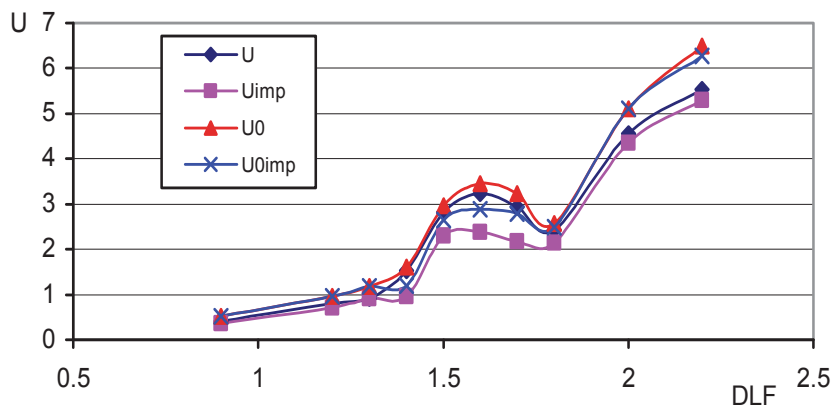

Fig. 13. The different deflections non-dimensional in function of DLF for column at length l = 200 mm

The shape of all the curves shown in Fig. 13 is similar, but the curves for which deflection was determined from overall displacements of a given point on the girder (including plate deflection and rotational displacement) are higher (with greater deflection values for the same DLF levels). The differences in maximum deflections determined from deflections measured only during the pulse time ($0 < t < T_p$) or throughout the entire time of response analysis ($0 < t < 1.5\ T_p$) occur for DLF in the range 1.2 to 2.0. Therefore, it is sufficient to analyze the maximum values of overall deflections during the pulse time as a function of DLF – U_{0imp} curve (DLF) – it is not necessary to take recourse to equation (3). The above confirms the fact that critical DLF values determined from the curves in Fig. 13 using the known criteria are the same, respectively.
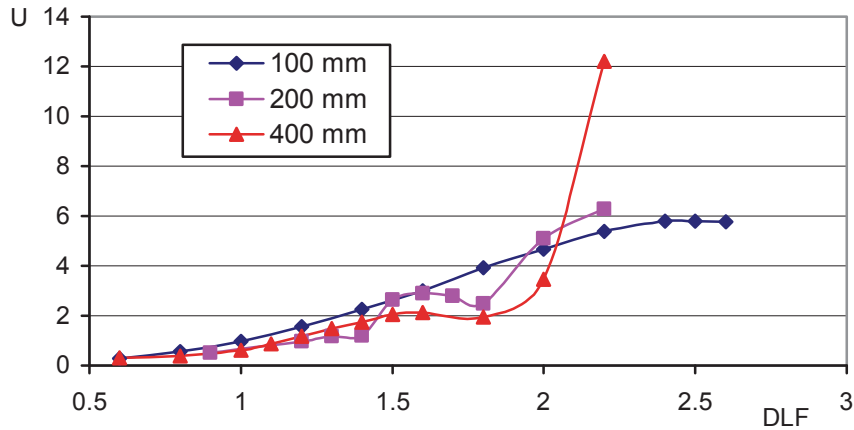

Fig. 14. The influence of column length on non-dimensional deflections in function of DLF

Furthermore, the influence of girder length on the critical values of the dynamic load factor was analyzed. Curves showing the relationship between the maximum deflections U of the selected point on the girder wall and the dynamic load factor DLF for girders of different lengths ($l = 100$, 200 and 400 mm) are presented in Fig. 14. Using the curves shown in Fig. 14 and the criteria given in the literature [5], the critical values of dynamic buckling were determined and presented in Tab. 2.

Tab. 2. Critical values of DLF and pulse amplitude $(T_a)_{or}$ determined using different criteria for girders of various lengths

	Volmir	Budiansky-Hutchnison	Ari-Gur and Simonetta
$l = 100$ mm	$DLF_{kr} = 1$ $(T_a)_{kr} = 4313$ Nm	$DLF_{kr} = 1.4 - 1.5$ $(T_a)_{kr} = 6038 - 6470$ Nm	-
$l = 200$ mm	$DLF_{kr} = 1.2$ $(T_a)_{kr} = 3091$ Nm	$DLF_{kr} = 1.4 - 1.5$ $(T_a)_{kr} = 3606 - 3864$ Nm	$DLF_{kr} = 1.6$ $(T_a)_{kr} = 4121$ Nm
$l = 400$ mm	$DLF_{cr} = 1.15$ $(T_a)_{kr} = 2420$ Nm	$DLF_{cr} = 1.2 - 1.3$ $(T_a)_{kr} = 2526 - 2736$ Nm	$DLF_{cr} = 1.5$ $(T_a)_{kr} = 3158$ Nm

Comparing the curves presented in Fig. 14 and the numerical results shown in Tab. 2, one can see that the critical values of the dynamic load factor DLF_{kr} are similar for the cases analyzed. However, it should be noted that the dynamic load factor is a dimensionless value, so the critical

values of the pulse loading amplitude are different for girders of different lengths, which is confirmed by the numerical results given in Tab. 2. Taking the above into consideration, it is apparent that with increasing girder length, the critical pulse loading amplitude decreases.

4.3. Summary of both methods used for dynamic stability assessment

In the previous sections of the paper, dynamic buckling was analyzed based on measurements of the angle of rotation or deflection of girder walls. The use of analysis of the rotation angle as a function of DLF was motivated by the fact that the literature on the subject refers to this value – that is, to the angle of rotation – in studies concerning torsional cases. For the sake of comparison, information was collected about the angle of rotation and wall deflection for different DLF values and one such case was compared and presented in Fig. 15, which shows a change in deflection (Fig. 15a) and in the angle of rotation (Fig. 15b).
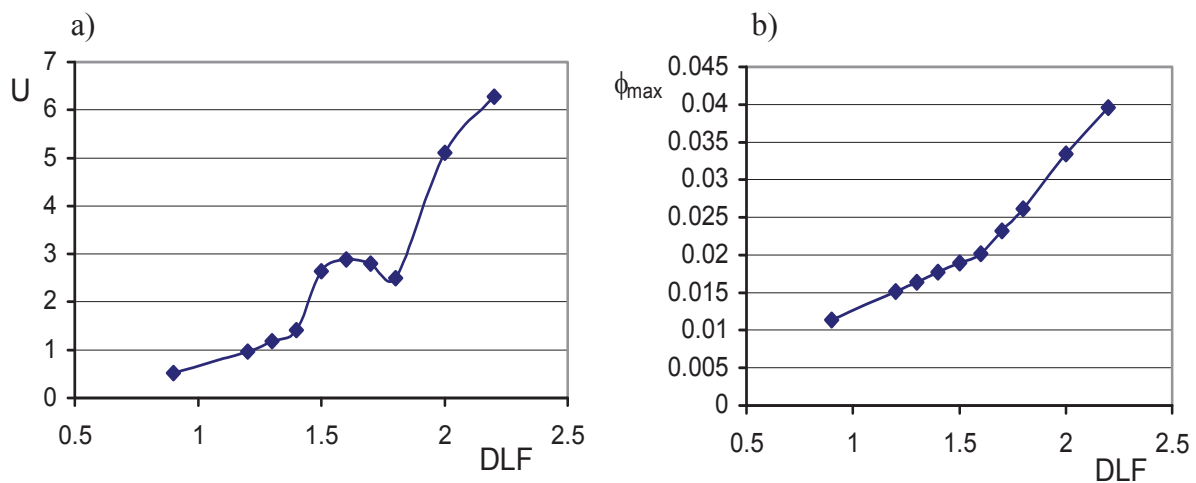

Fig. 15. The nondimensional deflections vs. DLF (a) and the rotation angle (b) for columns at length l = 200 mm

It would seem that both of these methods of analysis should yield similar results. However, this is not the case, primarily due to the fact that the angle of rotation rises with increasing DLF, which is not always true of changes in deflection. As Fig. 15a shows, there are some cases in which deflection may decrease with increasing dynamic load factor, which is most often related to a change in buckling mode. In plotting curves for deflection as a function of DLF, one can use not only the Budiansky-Hutchinson criterion, but also the Volmir criterion, as well as the criteria proposed for plates by Ari-Gur and Simonetta. The application of the last two criteria is impossible, if the angle of rotation is analyzed as a function of DLF.

In summary, analysis of the deflection of girder walls as a function of the dynamic load factor is more useful due to the known geometric criteria related to the curve representing the angle of rotation as a function of DLF for flat-walled girders. However, investigation of the maximum angle of rotation makes it possible to asses the load-bearing capacity of the whole structure rather than the local capacity (in random places where the deflection increases). For shells or pipes subjected to torsion, the angle of rotation–DLF curves may be sufficient, but to confirm this, one should conduct a number of analyses for shell structures including cylindrical shells.

5. Final remarks and conclusions

The paper presents the results of numerical calculations for girders subjected to torsion. Analysis was conducted through the transient application of loading to a given structure and the determination of its behaviour throughout the pulse duration. In the case of torsion, the criteria for

dynamic stability assessment have not been determined in the literature to date, so the presented methods of determining dynamic critical loads for box girders subjected to torsion constitute a novel concept. However, the authors would like to stress the appearance of a sharp increase in the angle of rotation or deflection for a given dynamic load, which may be, in their subjective assessment, the critical load, and, consequently, the static load.

The authors do realize that the best method of verification of the above findings would be to conduct an experimental study.

References

[1] Ari-Gur, J., Simonetta, S. R., *Dynamic pulse buckling of rectangular composite plates*, Composites Part B, 28B, pp. 301–308, 1997.

[2] Biskupski, J., Kołakowski, Z., *Stability of thin-walled box girders subjected to bounded torsion*, Engineering Machines Problems 3 (3), pp. 57-72, 1994.

[3] Graves-Smith, T. R., Sridharan, S., *A finite strip method for the buckling of plate structures under arbitrary loading*, International Journal of Mechanical Science, 20, pp. 685-693, 1978.

[4] Królak, M., Kubiak, T., Kołakowski, Z., *Stability and Load Carrying Capacity of Thin-Walled Orthotropic Poles of Regular Polygonal Cross-Section Subject to Combined Load*, Journal of Theoretical and Applied Mechanics, 4 (39), pp. 969-988, 2001.

[5] Kubiak, T., *Criteria for dynamic buckling estimation of thin-walled structures*, Thin-Walled Structures, 45 (10-11), pp. 888-892, 2007.

[6] Mania, R., Kowal-Michalska, K., *Behaviour of composite columns of closed cross-section under in-plane compressive pulse loading*, Thin-Walled Structures, 45, pp. 902–905, 2007.

[7] Ma, H. W., Zhang, S. Y., Yang, G. T., *Impact torsional buckling of plastic circular cylindrical shells experimental study*, International Journal of Impact Engineering, 22 (5), pp. 49-64, 1999.

[8] Petry, D., Fahlbusch, G., *Dynamic buckling of thin isotropic plates subjected to in-plane impact*, Thin-Walled Structures, 38, pp. 267–283, 2000.

[9] Wang, D. Y., Chen, T. Y., *Impact buckling and post-buckling of elasto-viscoplastic cylindrical shell under torsion*, China Ocean Engineering, 11 (1), pp. 43-52, 1997.

[10] Xinsheng, Xu, Jianqing, Ma, Lim, C. W., Zhang, G., *Dynamic torsional buckling of cylindrical shell*, Computer and Structures, 88, pp. 322-330, 2010.

[11] Zhang, X. Q., Han, Q, *Buckling and post-buckling behaviours of imperfect cylindrical shells under torsion*, Thin-Walled Structures, 45 (12), pp. 1035-1043, 2007.

[12] Supporting materials for Ansys 11.0 and Ansys 12.0.